

DUAL MODE FRACTURE BASED ON LOADING RATE DURING SLIDING INDENTATION OF Si-C-N HARD COATINGS ON 304SS SUBSTRATES

A.S. Bhattacharyya^{1, 2 §}

¹Department of Metallurgical and Materials Engineering, Central University of Jharkhand, Ranchi: 835205, India

²Centre of Excellence in Green and Efficient Energy Technology (CoE GEET) Central University of Jharkhand, Ranchi: 835205, India

[§]Corresponding author:

2006asb@gmail.com, arnab.bhattacharya@cuja.ac.in

ABSTRACT

Scratch tests were performed on thermal resistant hard Si-C-N coatings deposited on steel (SS) 304, by RF (Radio frequency) magnetron sputtering. The abrasion and wear properties were studied by analyzing the changing failure complexion inside the scratch showing a mixture of ductile and brittle properties. The change in loading rate caused noticeable changes in the failure mode. The plasticity was found to have a peripheral domination initially with increase in load but was replaced by brittle failure on increasing the loading rate. The work of adhesion and wear rate were determined.

Keywords: Scratch, hard coating, Si-C-N, loading rate, wear

INTRODUCTION

Being initially discovered as a polymer derived ceramic, Si-C-N coatings have been quite useful at high temperatures [1]. They act as barrier to high temperature and chemical degrading effects of the environment, protecting the substrate beneath [2, 3]. The presence of oxygen makes Si-C-N compatible with structural components like stainless steel due to the formation of Si-O-CN phase [4]. Protection against wear and abrasion is also one of the primary features of any hard coating [5]. However, an increase in hardness in some cases may cause embrittlement i. e. lower fracture toughness. Si-C-N coating has an edge over its counterparts as it does not lose its fracture toughness property even after getting sufficiently hard [6]. This attributes to the growth of very small crystallites in a mostly amorphous matrix causing deflections in the direction of propagation of any crack which might have generated [7]. The investigations on the fracture-based properties of Si-C-N coatings have been performed mainly with static indentations with the focus being kept on the stress distribution beneath the indentation region [8-12]. Considering the nature of load a structural component like stainless steel is exposed to, sliding indentations to analyse the fracture taking place will reveal some significant aspects in congruence with the wear and abrasion resistive properties. A similar study for nano scratch tests using a Berkovich indenter has been done earlier which are more useful for microelectronic devices [13]. The micro-scale approach has been presented related to heavy duty usage like automobiles, aerospace, reactors etc.

MATERIALS & METHODS

Si-C-N coatings were deposited on SS 304 substrates by magnetron sputtering (HHV, Bangalore, India) at 300°C at 400 W power and 1×10^{-2} mbar pressure in Ar/N₂ atmosphere from SiC target on stainless steel (SS304). The sliding

indents were carried out by Scratch Test Tr-101 (Ducom, Bangalore, India) that used a Rockwell C indenter which is a 120° diamond cone with 0.2mm diameter spherical tip. The scratch tests were done at rate of **20, 5 and 2 N/mm** at a speed of **0.2 mm/s**. The critical load (L_c) was determined from the point of change of slope in the coefficient of friction vs. normal load, tractional force, and scratch length curves. ImageJ software was used to get profiles of the scratch tracks.

RESULTS & DISCUSSIONS

The load vs. scratch length and coefficient of friction (c.o.f) vs. normal load curves obtained during tests on coatings placed on SS304 substrates for three distinct loading rates are shown in **Figs. 1-3**. Three factors mainly contribute to the scratching activity: (1) ploughing; (2) friction; and (3) stress. The increasing ploughing of the sample by the tip with increasing normal load is related to the constant increase in the coefficient of friction during scratching. The indentation stress and the flow stress on the coating which are the major parameters of the plough also increase with the increase in normal applied sliding load **[14]**. Coating removal occurs after coating failure, as evidenced by the shift in scratch track in the micrograph, which shows piling ups at the borders of the scratch. In the scratch test, the stress field is a mixture of Boussinesq (σ_{Bous}) owing to indenter loading, which has two components, normal and tangential, and Blister ($\sigma_{Blister}$) due to residual stress. The normal component of Bous is substituted with Hanso's field (σ_{Hans}) in conical indenters, causing radial fissures. These primary stresses are also related with shear components, as shown in **eq 1a, b**, where the superscripts n, t, and r signify "normal", "tangential", and "residual". **[15, 16]**.

$$\sigma = \sigma^n_{Hans} + \sigma^t_{Bous} + \sigma^r_{Blister} \quad (1a)$$

$$\tau = \tau^n_{Hans} + \tau^t_{Bous} + \tau^r_{Blister} \quad (1b)$$

A complete brittle failure is evident from the formation of debris and spallation occurring due to the interaction of the radial and lateral cracks. A matter of deformation scale is evident from these observations as lowering the load increases the probability of ductile fracture. An increased brittleness has been reported to be indirect evidence of the lowering of adhesion **[17]**. The tractional force curve **Fig 1(a)** shows a sudden and prominent slope change at **23N** which is the critical load (L_c) where adhesive failure with μ_{eff} around **0.32** (**Fig 1b**) **[12]**. L_c is related to the work of adhesion (W) as given in **eq 2**, where E is the modulus, d_c is the width of the scratch track at critical load and t is the thickness of the coating. The nature of substrate also affects the adhesion as lower L_c is found for amorphous substrates and higher values for crystalline metal substrates **[18]**.

$$L_c = \frac{\pi d_c^2}{8} \left[\frac{2EW}{t} \right]^{\frac{1}{2}} \quad (2)$$

The scratch track is shown in **Fig 1c** and the profiles of the regions marked are shown in **Fig 1d to h**. The scratch width was found as **150 μm** . The coatings were about **2.5 μm** thick and having an elastic modulus of **220 GPa**. The work of adhesion using **eq 2** comes out as **0.038 nJ/m²**. The scratch track consisted of high pile up of **250 μm** along the sides. As the indenter diameter was 200 mm, the cylindrical sides were involved in the scratching event causing the pileup. The central groove in the scratch track was due to the plastic deformation and showed pile up coming from the 304SS substrate beneath. The pile up was about **75 μm** from the track (**Fig 1d**). A change in the nature of the track is clearly visible as marked by a square, where the central groove region changed resembling a ductile to brittle transition. We can denote this point as the region of initiation of fracture. The material loss in the mid regions showed an increase as the scratching continued while the pile ups were comparatively less (**Fig 1 e, f**). The delamination region of **60 μm** width and **75 μm** height gets merged with the piled-up segments. The ductile failure was dominant in the initial stages of the scratch with a small central pileup region of **45 μm** (**Fig 1g**). A sudden increase of about **12 μm** (Δh) due to material removal took and can be used to find the wear rate. The specific wear rate WR_s is given as **eq 3a**, which is equivalent to **eq 3b**. The denominator can also be replaced by $R_L (\Delta l)^2$ where R_L is the load rate (**5N/mm**) and Δl is the scratch distance for which the sudden change Δh occurred as shown in the **Fig 1h**.

$$WR_s = \frac{\text{Volume Loss}}{\text{Load} \cdot \text{sliding distance}} \quad (3a)$$

$$WR_s = \frac{(\Delta h)^3}{L_c \cdot (\Delta l)} = \frac{(\Delta h)^3}{R_L \cdot (\Delta l)^2} \quad (3b)$$

A loading rate of **20 N/mm** showed higher substrate influence evident from the comparatively lower slopes of the tractional force curves during the scratching process and formation of two critical loads (**Fig 2a**). The lower critical load was **16 N** while the upper critical load was **21 N**. The dual critical loads are evidence of higher percentage of ductile failure taking place not causing any sudden change in material removal. The μ_{eff} was also higher (**0.44**) as shown in **Fig 2b**. The upper critical load of **21N** was determined from intersection of two tangents from the two regions.

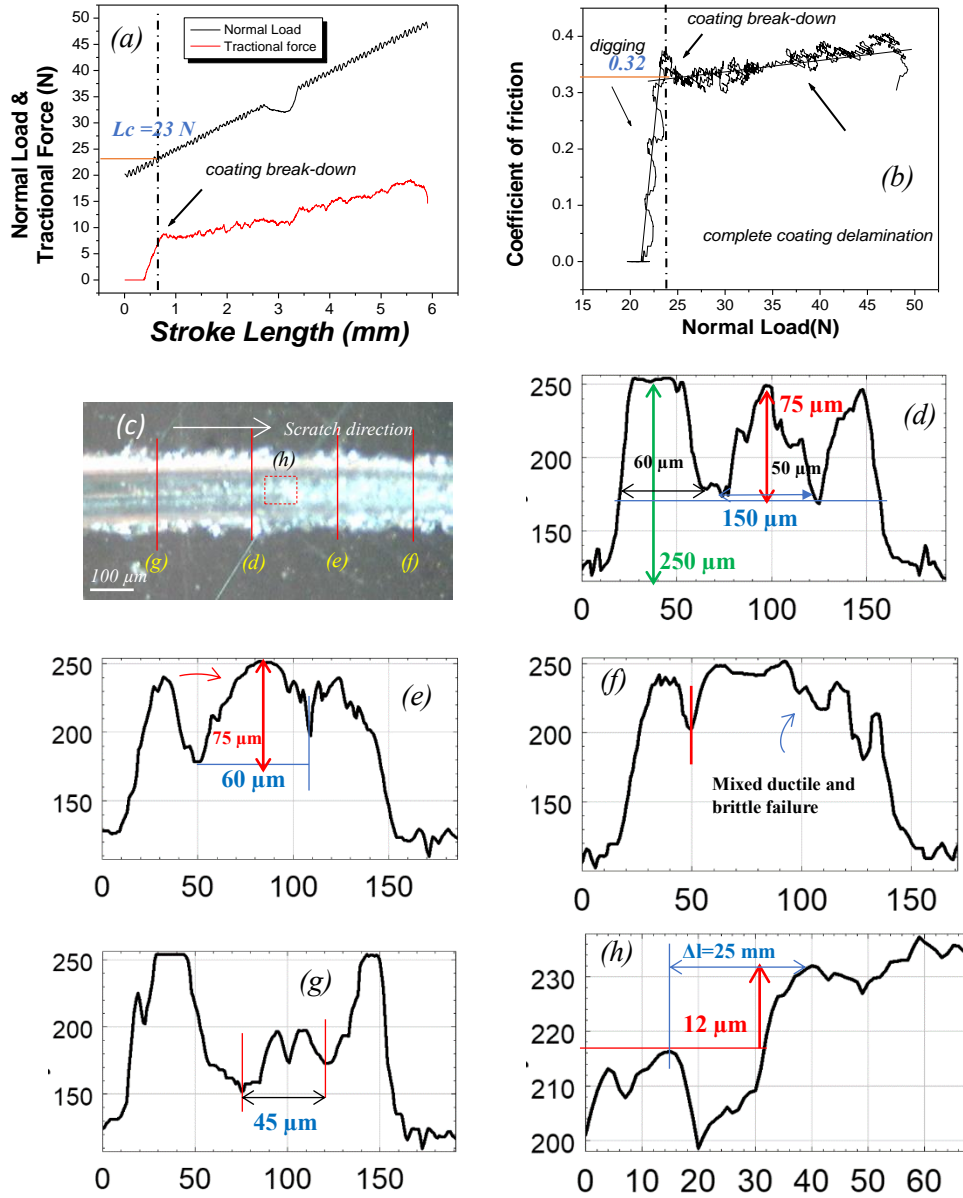


Fig 1: Scratch tests with 5N/mm loading rate for steel substrates showing plots of (a) Normal load and Tractional force vs stroke length, (b) C.O.F vs normal load and (c) the optical micrograph of the scratch track (**reproduced with permission**) [12] (d-h) profiles of the regions marked in (c).

The scratch track did not show any fracture process confined inside the scratch track, rather *Hertzian* cracks can be seen at higher loads indicating cohesive failure (**Fig 2c**) [12]. Formation of a sharp and narrow groove region experiencing pile up can be seen from the profile (**Fig 2d**) accompanied by pile ups as in the previous case. At higher loads, the central groove got replaced by brittle failure as evident from the multiple peaks of similar height and width (**Fig 2e**). The brittle failure got intensified as the multiple peaks started to merge indicating coating removal. A height change of 20 μm for 8 mm was found

The adhesive failure for the scratch in **Fig 3a** occurred at a critical load is **21 N** and 0.27 as μ_{eff} (**Fig 3b**) for the lowest loading rate of **2N/mm**. The central scratch groove was observed all throughout the scratch length (**Fig 3c**) [12]. The line profile however showed an increased central pile up with load with the peak height increasing from **60 μm** to **120 μm** without any significant change in groove width (**6 μm**) (**Fig 3d, f, g**). No central groove was seen for a certain portion of the scratch track which is most probably due to strain hardening (**Fig 3e**). No pile ups were found at the sides of the scratch track. Adhesive failure occurred at a stroke length of **4 mm** which is evident from the sudden rise in the tractional force curve which also shows the release of stored elastic energy. A summary of the observations made with the change in loading rate is given in **Table 1**. The pile up has been represented as height to width ratio prior to any adhesive failure in the peripheral region and in the central groove region. Then Rockwell C indenter used has a spherical tip of diameter **200 μm** . Therefore, for a load of **23 N**, the stress imposed will be **732 MPa** and **669 MPa** for the other two cases. The determination of wear shall therefore require it different approaches for the different loading rates. For 2N/mm loading rate, it will be the groove (h/w) aspect ratio $\times (\sigma_c)^{-1}$, which is equal to **0.0137 mm^2/N** . For the other two loading rates, both the groove and side pileup (h/w) aspect ratios has been considered. The lowest wear rate was obtained for a loading rate of **5N/mm**.

Table 1. Effect of loading rate on the scratch track features

R_L (N/mm)	pile up (h/w)	Groove (h/w)	L_c (N)	σ_c (MPa)	WRs $\times 10^{-3}(\text{mm}^2/\text{N})$	Nature of Failure	Special features
2	nil	10	23	732	13.7	Mostly Ductile	Strain hardening
5	4.17	1.5	21	669	8.5	Ductile to Brittle	Fracture inside with pile up at the periphery
20	11.12	1.33	21	669	18.6	Ductile –Brittle-ductile	Hertzian cracks

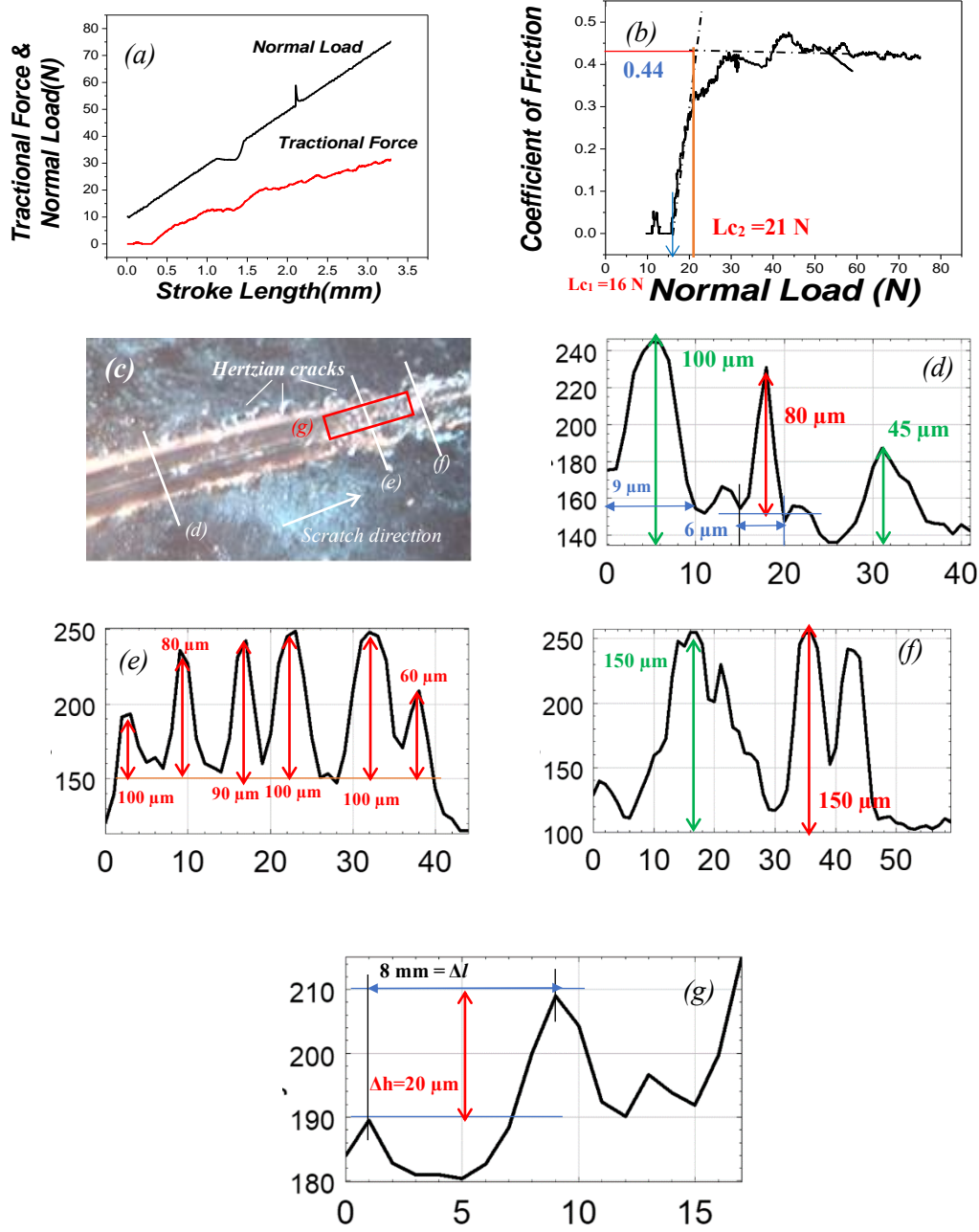


Fig 2: Scratch tests with **20N/mm** loading rate for Silicon substrates showing plots of **(a)** Normal load and Tractional force vs stroke length, **(b)** C.O.F vs normal load and **(c)** the optical micrograph of the scratch track (**reproduced with permission**) [12] **(d-g)** profile of the marked regions in (c)

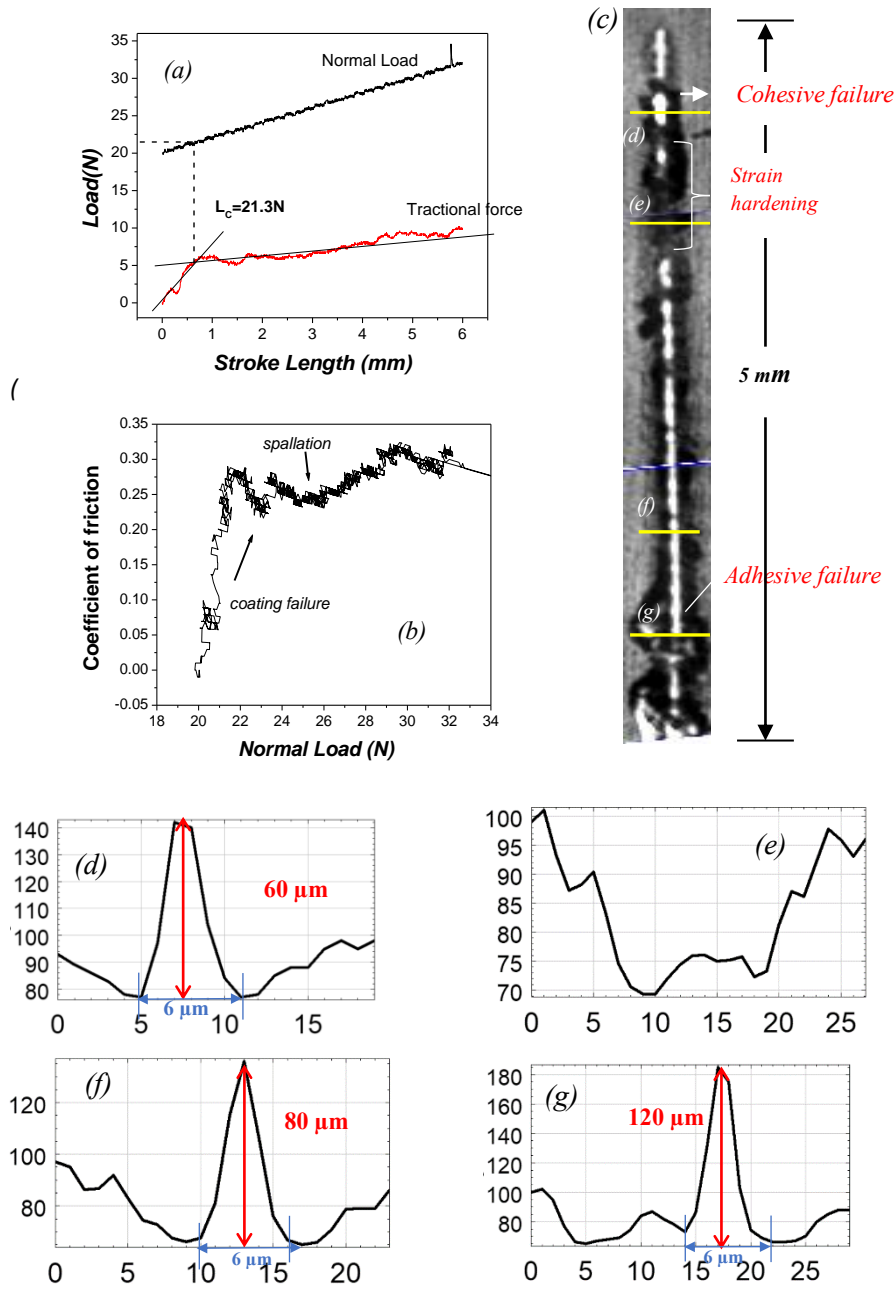


Fig 3: Scratch tests with 2N/mm loading rate for steel substrates showing plots of **(a)** Normal load and Tractional force vs. stroke length, **(b)** C.O.F vs. normal load and **(c)** the optical micrograph of the scratch track **(reproduced with permission)** [12] **(d-g)** profile of the marked regions in (c)

CONCLUSIONS

Scratch tests were performed on Si-C-N hard coatings deposited in (SS) 304 stainless steel substrates. High plasticity was observed for a low rate of **2N/mm** with strain hardening. Although an initial increase in loading rate from **2 to 5N/mm** made the failure more brittle inside the scratch track, with disappearance of the central groove at higher loads and abrupt change in material removal, plasticity was however still prevalent at the sides with high amount of pile ups taking place. The nature of fracture went back to having an overall higher ductility percentage at **20N/mm** compared to 5N/mm with appearance of lower and upper critical loads. The formation of Hertzian circular cracks being typical for cohesive failure was observed only at **20N/mm**. So, it can be said that with increase in loading rate, the plasticity or ductility deviates and moves to the peripheral region of the scratch tracks. A novel way of determination of specific wear rate through scratch tests was also presented. The lowest wear rate was obtained for **5N/mm** loading. Also, the coating should be developed and subjected to external loads in such a way that its ductile and brittle features are co-existent for improved fracture and wear resistance.

ACKNOWLEDGEMENTS

The author hereby thanks Dr. S. K. Mishra for experimental studies

DECLARATIONS

Compliance with Ethical Standards

The manuscript has not been submitted in parallel either in full or partially to any other journal.

Conflict of interest

There is no conflict of interest among the authors

Research Data Policy and Data Availability Statements

Data shall be provided on request

Credit author statement

A. S. Bhattacharyya being the sole author, was involved in performing the experiments, analysing, and framing the manuscript

FUNDING

No funding was received for conducting the research

REFERENCE

1. Riedel, R.; Kleebe, H.-J.; Schönfelder, H.; Aldinger, F. A Covalent Micro/Nano-Composite Resistant to High-Temperature Oxidation. *Nature* 1995, 374 (6522), 526–528. <https://doi.org/10.1038/374526a0>.
2. A.S. Bhattacharyya, G.C. Das, S. Mukherjee, S.K. Mishra, Effect of radio frequency and direct current modes of deposition on protective metallurgical hard silicon carbon nitride coatings by magnetron sputtering, *Vacuum*, 83, 12, 2009, 1464-1469, <https://doi.org/10.1016/j.vacuum.2009.06.051>.
3. Mishra, S. K.; Bhattacharyya, A. S.; Rupa, P. K. P.; Pathak, L. C. XPS Studies on Nanocomposite Si–C–N Coatings Deposited by Magnetron Sputtering *Nanoscience and Nanotechnology Letters*, 4, 3, 2012, 352-357 <https://doi.org/10.1166/nml.2012.1320>
4. H. J. Choi, K. Lu, A high compatibility SiOCN coating on stainless steel. *Journal of Materials Science* (2023) 58, 3790 <http://dx.doi.org/10.1007/s10853-023-08252-6>
5. S.K. Mishra, A.S. Bhattacharyya, P. Mahato, L.C. Pathak, Multicomponent TiSiBC superhard and tough composite coatings by magnetron sputtering, *Surface and Coatings Technology*, 207, 2012, 19-23, <https://doi.org/10.1016/j.surfcoat.2012.03.047>.

6. Tomastik, J.; Ctvrtlik, R.; Ingr, T.; Manak, J.; Opletalova, A. Effect of Nitrogen Doping and Temperature on Mechanical Durability of Silicon Carbide Thin Films. *Sci. Rep.* 2018, 8 (1). <https://doi.org/10.1038/s41598-018-28704-3>.
7. Bhattacharyya, A. S.; Kumar, R. P.; Priyadarshi, S.; Sonu, Shivam, S.; Anshu, S. Nanoindentation Stress–Strain for Fracture Analysis and Computational Modeling for Hardness and Modulus. *J. Mater. Eng. Perform.* 2018, 27 (6), 2719–2726. <https://doi.org/10.1007/s11665-018-3289-7>.
8. R. Dash, K. Bhattacharyya, A.S. Bhattacharyya, Film failure at earlier and later stages of nanoindentation in static and sliding mode. *Eng Fail Anal* (2023) 150, 107353 <https://doi.org/10.1016/j.engfailanal.2023.107353>
9. R. Dash, K. Bhattacharyya, A. S. Bhattacharyya. Fracture associated with static and sliding indentation of multicomponent hard coatings on silicon substrates, *Fatigue & Fracture of Engineering Materials & Structures* (2023) 46: 1641-1645. <https://doi.org/10.1111/ffe.13960>
10. R. Dash, R. P. Kumar, K. Bhattacharyya, A. S. Bhattacharyya, Intensified chipping during nanoindentation and the effect of friction on the interfacial fracture for thin films used in N/MEMS, *IOP- Engineering Research Express*, 2022 4 045012 <https://doi.org/10.1088/2631-8695/ac9c85>
11. Sun, L.; Ma, D.; Wang, L.; Shi, X.; Wang, J.; Chen, W. Determining Indentation Fracture Toughness of Ceramics by Finite Element Method Using Virtual Crack Closure Technique. *Eng. Fract. Mech.* 2018, 197, 151–159. <https://doi.org/10.1016/j.engfracmech.2018.05.001>.
12. Mishra, S.K., Bhattacharyya, A.S. (2013). Adhesion and Indentation Fracture Behavior of Silicon Carbonitride Nanocomposite Coatings Deposited by Magnetron Sputtering. In: Li, H., Wu, J., Wang, Z. (eds) *Silicon-based Nanomaterials*. Springer Series in Materials Science, vol 187. Springer, New York, NY. https://doi.org/10.1007/978-1-4614-8169-0_10
13. A.S. Bhattacharyya. Sliding indentation: Failure modes with study of velocity and loading rate, Surface Topography: Metrology and Properties 2021 *Surf. Topogr.: Metrol. Prop.* 9 (2021) 035052 <https://doi.org/10.1088/2051-672X/ac28aa>
14. Bharat Bushan, B.K. Gupta, Handbook of Tribology (Materials Coatings and Surface Treatments) 15.45- 15.58 ISBN0-07-005249-2.
15. Qian, H.; Chen, M.; Qi, Z.; Teng, Q.; Qi, H.; Zhang, L.; Shan, X. Review on Research and Development of Abrasive Scratching of Hard Brittle Materials and Its Underlying Mechanisms. *Crystals* 2023, 13, 428. <https://doi.org/10.3390/cryst13030428>
16. Lv, B.; Lin, B.; Sui, T.; Liu, C. Crack Extension Mechanism and Scratch Stress Field Model of Hard and Brittle Materials Caused by Curvature Effect. *J. Mater. Process. Technol.* 2023, 319 (118058), 118058. <https://doi.org/10.1016/j.jmatprotec.2023.118058>.
17. Kabir, M. S.; Zhou, Z.; Xie, Z.; Munroe, P. Scratch Adhesion Evaluation of Diamond like Carbon Coatings with Alternate Hard and Soft Multilayers. *Wear* 2023, 518–519 (204647), 204647. <https://doi.org/10.1016/j.wear.2023.204647>.
18. S.J. Bull, E.G. Berasetegui, An overview of the potential of quantitative coating adhesion measurement by scratch testing, *Tribol. Int.* 39 (2006) 99–114. [10.1016/S0167-8922\(06\)80043-X](https://doi.org/10.1016/S0167-8922(06)80043-X)